Revista Brasileira de Geofísica

RBGf

Brazilian Journal of Geophysics

PETROPHYSICAL CHARACTERIZATION OF ALBIAN CARBONATE RESERVOIR IN CAMPOS BASIN (BRAZIL) USING A MULTIVARIATE APPROACH WITH WELL LOGS AND LABORATORY MEASUREMENTS

Abel Carrasquilla[1] and Raphael Ribeiro Silva[2]

ABSTRACT. This study characterizes an Albian carbonate reservoir of Field B in the Campos Basin (Brazil), based on geophysical well logs and laboratory petrophysical data. This permitted us to estimate the porosity, permeability and water saturation of this reservoir more reliably. In order to achieve this goal, the Cluster Analysis for Rock Typing module of the Interactive Petrophysics software was used to divide the well into electrofacies. For each of them, an equation was determined to find the porosity and the permeability, using the multiple linear regression technique, using as input the log data and as target the laboratory data. The obtained results were compared with different models proposed by other authors, with the best results being found with multiple linear regression. Water saturation, on the other hand, was estimated by Archie Equation after identifying the cementation coefficient with the Pickett crossplot. Finally, the porosity and permeability data were again used to now identify three main flow units in the reservoir through the Winland graph. To verify the effectiveness of the adopted methodology, it was successfully applied in a blind test, defining porosity, permeability, water saturation and flow units in a well without laboratory data.

Keywords: well logging, Field B, petrophysics, carbonate reservoir, Albian.

RESUMO. Este estudo caracteriza um reservatório carbonático Albiano do Campo B na Bacia de Campos, a partir de dados de perfis de poço e de petrofísica de laboratório. Esta análise nos permitiu estimativas mais confiáveis de porosidade, permeabilidade e saturação de água. Com esse objetivo, foi usado o módulo *Cluster Analysis for Rock Typing* do software *Interactive Petrophysics* para dividir o poço em eletrofácies. Para cada uma delas, foi determinada uma equação para a porosidade e a permeabilidade, através da técnica de regressão linear múltipla, usando como entrada os dados de perfis de poço e como alvo os dados de laboratório. Esses resultados foram comparados com modelos propostos por outros autores, sendo os melhores aqueles obtidos com regressão linear múltipla. A saturação de água foi estimada com a Equação de Archie após identificar o coeficiente de cimentação com o *crossplot* de Pickett. Finalmente, os dados de porosidade e permeabilidade foram usados para identificar três unidades de fluxo através do gráfico de Winland. Para verificar a eficácia da metodologia adotada, a mesma foi aplicada com sucesso num teste cego, definindo a porosidade, a permeabilidade, a saturação de água e as unidades de fluxo num poço sem dados de laboratório.

Palavras-chave: perfis de poços, Campo B, petrofísica, reservatório carbonático, Albiano.

Universidade Estadual do Norte Fluminense, Laboratório de Engenharia e Exploração de Petróleo, LENEP/UENF, Av. Brennand s/n, Imboacica, Cx. Postal 119562, 27925-535 Macaé, RJ, Brazil. Phone/Fax: +55(22) 2765-6565 — E-mails: abel@lenep.uenf.br; raphael.otacon@gmail.com

INTRODUCTION

While some porosity and other physical properties are routinely evaluated from logs, the measurement in situ of permeability is usually not feasible at low cost, being made by formation tests. Furthermore, it is recognized that permeability is a property depending on the determining scale, so that its measurement on cores cannot be directly utilized for the valuation of the permeability in the reservoir scale. Therefore, the ability to estimate petrophysical properties of a reservoir rock from other more easily measured parameters or by means of laboratory tests is of great value to the petroleum industry. The petrophysical characterization using logs, for instance, is of capital importance to the discovery of new hydrocarbon reservoirs and aims to reduce the uncertainty and risks associated with oil exploration. Just as important are the early stage of development of an oilfield, helping to define the best development strategy through the petrophysical and geological characterization (Lucia, 1999).

So, logs and analysis of rock samples in the laboratory are methods widely used to evaluate the physical properties of geological formations in the petrophysical characterization of carbonate reservoirs (Aguilera & Aguilera, 2001). The data resolution and the spatial coverage in these two methods, combined with the number of measured parameters, occur in different ranges to obtain knowledge of the lithology and subsurface structural information (Shenawi et al., 2007). Therefore, the proposed study aims to explore the advantages of these two techniques, even adding the geological interpretation, to evaluate, from the petrophysical point of view, a dataset from a carbonate reservoir from Oilfield B in Campos Basin.

Geological Context

Campos is the most producing Brazilian oil basins, accounting for over 80% of national production (Fig. 1). In it there are fields with the presence of carbonate Albian reservoirs with medium porosity and permeability of 250 mD and 25%, respectively. These reservoirs are characterized as being heterogeneous materials, having a textural variety and are typically broken, which leads to a generally low recovery factor and complex relationship between the properties of the rock and geophysical data. For both, characterize carbonate reservoirs through a combination study of their petrophysical properties and their logs provides a fundamental understanding of its geometry and its dynamic properties (Bruhn et al., 2003).

This sedimentary basin is located along the continental margin of South Eastern Brazil, which has several oilfields (Fig. 1).

The origin and evolution of this basin are related to the Gondwana breakup and is marked by the breakup of South America and Africa plates with the subsequent formation of South Atlantic Ocean. The tectonic-sedimentary evolution of this basin occurred in three phases: rift, post-rift, and drift, that corresponds, respectively, to continental, transitional and marine super sequence. The continental sequence was deposited during the mechanical subsidence from the rift phase and includes the basalts of the Cabiunas Formation and continental sediments of the Lagoa Feia Formation. The transitional sequence is characterized by the evaporites of the Retiro Formation deposited in a period of shallow marine transgression pulses over continental areas and relative tectonic quiescence. The marine sequence marks the beginning of the open marine deposition during thermal subsidence associated with the drift phase. This stage begins with carbonate sedimentation (Macaé Group) and grade to a mainly siliciclastic succession (Campos Group) affected by intense halokinesis (Okubo et al., 2015).

METHODOLOGY

The methodology used in this study was as follows (Silva, 2016):

a) Initially, two wells were selected in this field, called X and Y, having the first well logs and laboratory petrophysical data and the second only logs. The well X was used as a reference and Y as a blind test, whereas the distance between them is small (180 m), which have similar geological characteristics.

b) Gamma ray, resistivity, sonic, density and neutronic porosity logs in the reference well X were interpreted by deriving petrophysical parameters such as porosity, permeability and saturation, which were compared with the same parameters measured in the laboratory, allowing a more reliable reservoir characterization.

c) These initial estimates were subject to statistical analysis using parameters such as maximum, minimum, average, median, mode, standard deviation, and histograms, which served to have a broader understanding of these petrophysical parameters.

d) Linear regression and multiple linear regression techniques were used to estimate both the porosity and permeability from neutron porosity, density, sonic, exploiting its linear dependence of porosity.

e) Cluster Analysis for Rock Typing module of Interactive Petrophysics software (LR Senergy, 2014) was employed
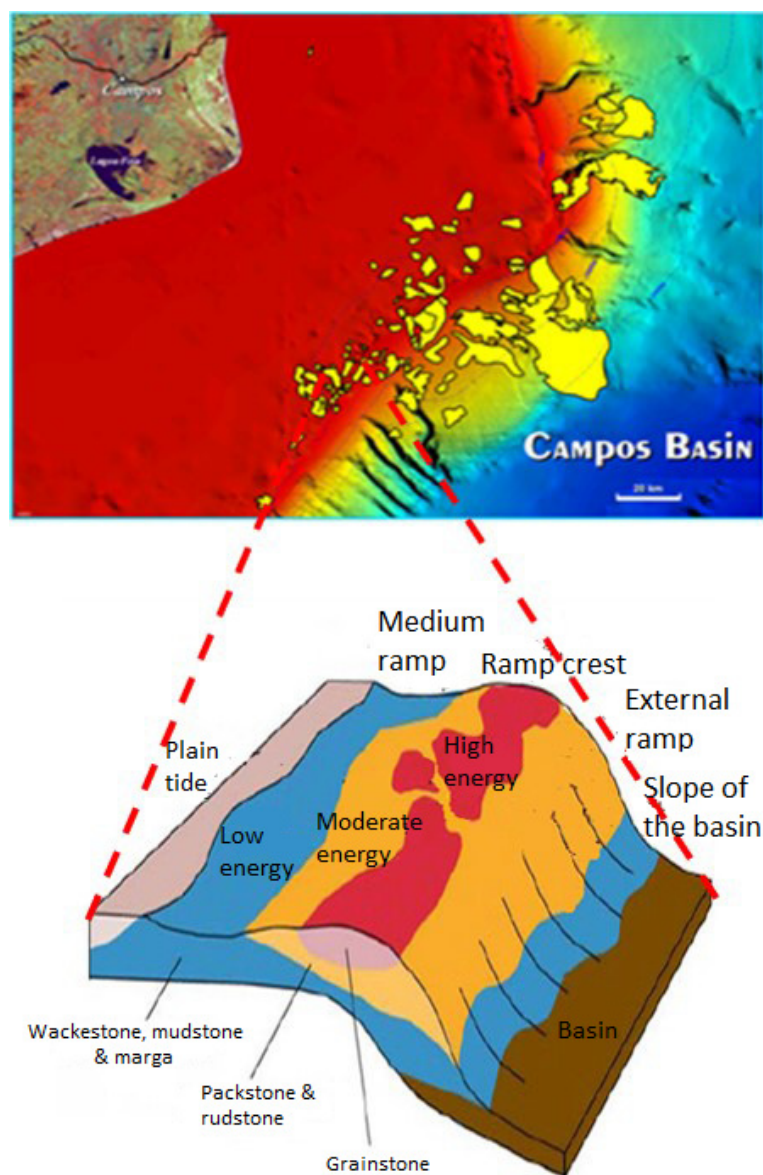
Figure 1 – Albian carbonate reservoirs in Campos Basin (modify from Bruhn et al., 2003).

to estimate porosity and permeability values aiming at a better correlation with laboratory data.

f) Cross-correlation, Pickett and Winland graphs were constructed to serve the initial interpretation, helping in determining electrofacies, location of flow areas and better adjusting with laboratory parameters.

g) Finally, all the methodology applied to the well reference X was used to infer the same petrophysical parameters in a blind test, nearby well Y, which lacked laboratory data.

RESULTS

The plotted histograms for the logs indicate gamma and resistivity ray logs have distorted right to low distribution. Density, neutron porosity and sonic logs have unimodal or symmetric distribution, which has centralizing behavior data with mean and standard deviation as a normal distribution (Fig. 2). The asymmetric distribution may be influenced by the presence of geological formations with low resistivity and high radioactive content, such as shales and/or clays. As density, neutron porosity and sonic logs are really connected to the porosity estimation, the symmetrical
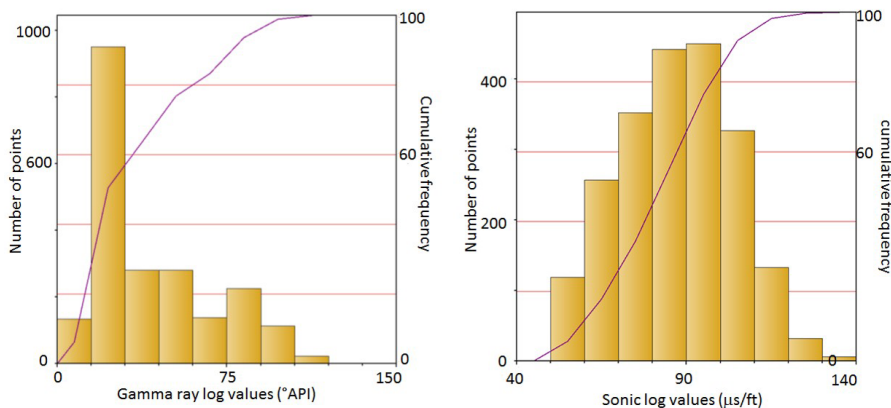
Figure 2 – Histograms of gamma rays (left) and sonic (right) logs of well X – Oilfield B.

distribution may be indicating the presence of micro, macro and meso porosities. Among the statistical values that are shown in Table 1, we can highlight the high standard deviation of the resistivity log (148.100 ohm.m), which indicates that it is the log with more uncertainty in its measurement. The values of 40.516, 30.065, 2.321 and 22.226 are the average or the quantity of central tendency for gamma ray, resistivity, density, neutron porosity and sonic logs, respectively. For mode or the value that appears most often in a set of data, the values of 16.484, 18.463, 2.352 and 94.605 are for the gamma ray, resistivity, density, neutron porosity and sonic logs, respectively.

Wells X and Y are spaced 1.36 km and well Y in a direction 32° east. From the data of the logs it is possible to correlate the wells. The correlation is presented in Figure 3, considering the logs in the zone of interest. By presenting the logs on the same scale, it is possible to conclude that the zone of interest in well X is deeper around 10 m than in well Y. In this figure, four main intervals with similar characteristics between the logs are identified:

1) high resistivity, density log to the left of the neutron curve and higher values of sonic. These features point the presence of hydrocarbons;

2) the values of the resistivity log and the falling of sonic log, indicating a transition zone;

3) the resistivity and the distance between the density and neutron curves indicate a zone of water;

4) a small resistivity peak indicating a second zone with hydrocarbons, but the other logs indicate low porosity and permeability.

On the other hand, laboratory data display in Figure 4 a strong linear dependence between permeability and porosity, with a $R^2 = 0.81$ (Pearson Correlation Coefficient) and, a linear relationship equation in the form $\log(k_{LAB}) = -1.4142 + 7.2875_{\phi LAB}$ between these two parameters. The blue light indicates oil and the dark light is water. The porosity data measured in the laboratory vary between 0.7% and 35%, with the values

Table 1 – Statistical summary of the values of well X logs.

Log	Minimum	Maximum	Average	Medium	Mode	Standard deviation
Gamma Ray (°API)	11.203	116.824	40.516	29.421	16.484	26.610
Resistivity (Ω.m)	0.454	1801.438	30.065	1.923	18.463	148.100
Density (gr/cm³)	1.399	2.670	2.321	2.339	2.352	0.156
Neutron porosity (%)	0.671	45.332	22.226	22.637	21.662	7.905
Sonic (μseg/ft)	51.480	143.234	87.054	87.236	94.605	16.549
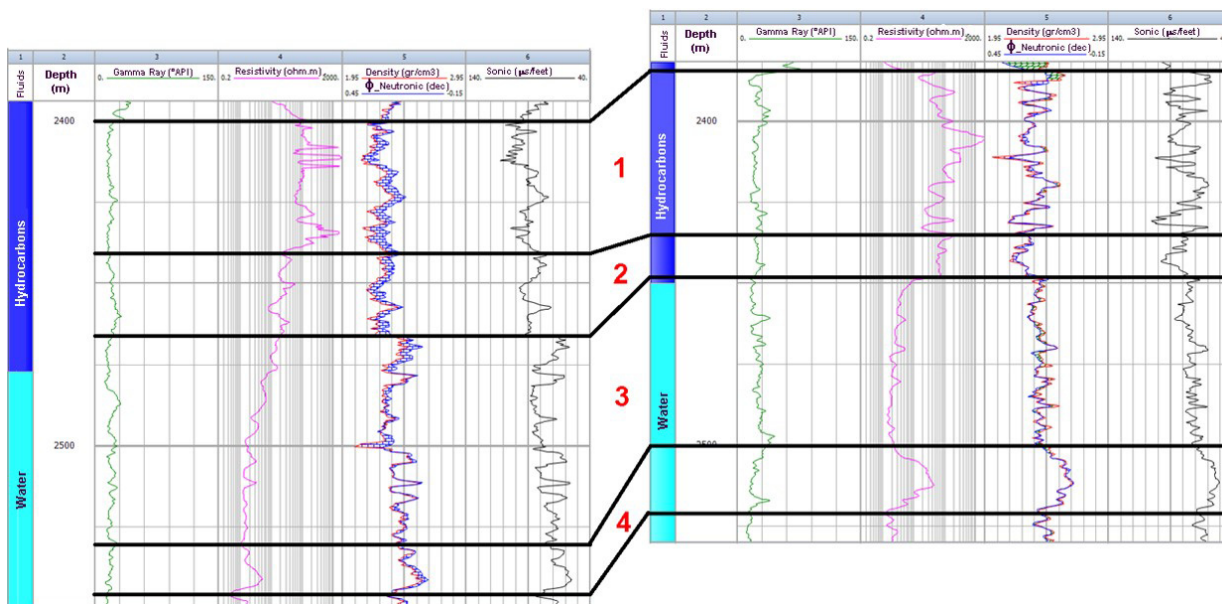
Figure 3 – Correlation between gamma ray, resistivity, density, neutron porosity and sonic logs to the wells X and Y of Oilfield B in Campos Basin. The red numbers 1 to 4 indicate areas with similar characteristics.


$$\log(k_{LAB}) = -1.4142 + 7.2875\phi_{LAB}$$

$$R^2 = 0.81$$
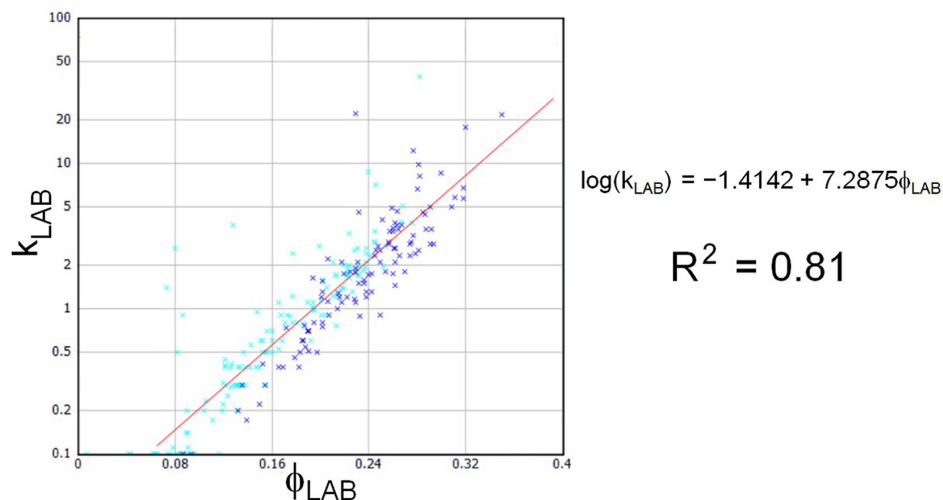
Figure 4 – Porosity (ϕ_{LAB}) and permeability (k_{LAB}) laboratory data crossplot for well X showing a strong direct relationship, with dark blue indicating the hydrocarbon zone and light blue the aquifer.

concentrating between 20% and 24%. In the identified oil section, the porosity is concentrated between 24% and 28%, while in the identified water piece the porosity is concentrated between 12% to 16% and 20% to 24%. The histogram shows a bimodal behavior but considering only the data of the oil unit the behavior is asymmetric to the left. Permeability data measured in the laboratory, the values are concentrated between 1.6 mD to 1.8 mD and range between 0.1 mD and 40 mD. In the identified hydrocarbon portion, the permeability is concentrated between 1.6 and

1.8 mD and, the histogram shows a symmetrical behavior. In the water section the permeability is concentrated around 0.3 mD to 0.5 mD and the histogram behaves bimodal. The behavior of the histogram with all the data is bimodal (Fig. 5).

The results of the clustering to density, neutron and sonic logs in wells X and Y have up to consolidate 20 groups (number of vertical lines at the base of the graph) and 10 electrofacies (different colors), according to the dendogram of Figure 6. A dendogram illustrates the information in the amalgamation
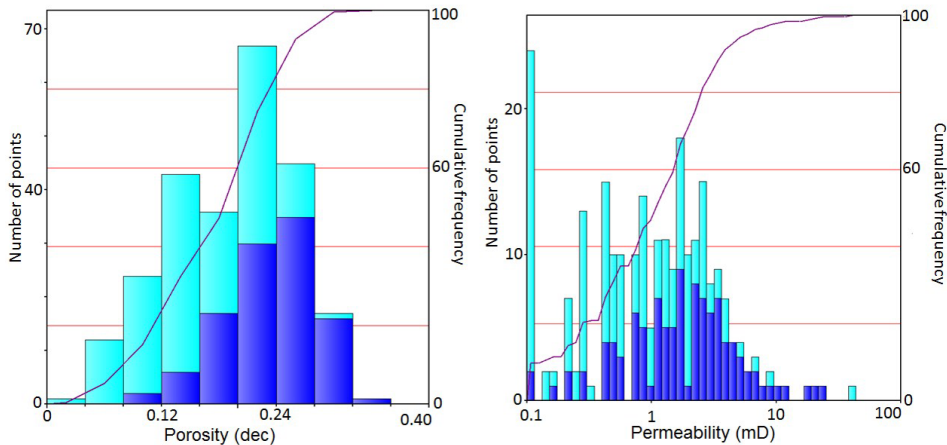
Figure 5 – Porosity (ϕ_{LAB}) and permeability (k_{LAB}) laboratory histograms for well X with dark blue indicating the hydrocarbon zone and light blue the aquifer.

table in the form of a tree diagram. By default, the level of similarity is measured on the vertical axis and the different observations are listed along the horizontal axis. Through the dendogram and prior knowledge about the data structure, a cutoff distance must be determined to define which groups will be formed. This decision is subjective and should be made according to the purpose of the analysis and the number of desired groups. In Figure 6, the first cut leaves 17 groups, but with the second cut, only 10 are allowed. Another way to choose the number of electrofacies is through the randomness ratio, as shown in Figure 7. The value of 10 electrofacies is chosen because it presents a reasonable ratio of, according this figure, but still guarantee a good amount of data groups, since carbonate rocks are heterogeneous. In Figure 8, the representation of this electrofacies in depth, the third track of the figure, whose values above 9 have the best reservoir characteristics. The determination of these electrofacies served as guidance to make a better estimate of the porosities and permeabilities derived from these logs (Fig. 9).

To the well X, when comparing with laboratory data, we observe fine adjustments to all estimates of porosity and permeability, but multiple linear regression resulted to be the best when compared with laboratory data (Fig. 9, left), for estimations derived density (track 3), neutron (track 4) and sonic (track 5) logs, and for effective (track 6) and multiple linear regression – MLR (track 7) evaluations. The effective porosity is expressed like this:

$$\phi_{EFF} = \phi_{TOTAL} - V_{SHALE}\phi_{SHALE}, \qquad (1)$$

where, ϕ_{EFF} is the effective porosity, ϕ_{TOTAL} is the total porosity, ϕ_{SHALE} is the shale porosity and V_{SHALE} is the shale volume. The expressions for MLR have the following

general form:

$$\phi_{MLR} = a + b\varrho_b + c\phi_N + d\Delta_t, \qquad (2)$$

where, ϕ_{MLR} is the MLR porosity, ρ_b is the density log, ϕ_N is the neutron porosity log, Δ_t is the sonic log and a, b, c and d are regression coefficients, which are stated each electrofacies in accord the Table 2. As can be seen in this figure, ϕ_{MLR} presents the best fit. But due to the value the of coefficient a, which represents a further regression coefficient, is larger than the coefficients b, c and d, which represent, respectively, the weight of ρ_b, ϕ_N and Δ_t logs, it can say that the adjustment is good but that it is more mathematical than physical.

In the case of permeabilities, Burrowes et al. (2010) and Tiab & Donaldson (2004) state that the exercise of the linear regression – LR technique between porosity and permeability is limited, since it delivers good results only in homogeneous formations, from the petrophysical point of thought, which is not the case for carbonate formations. Thus, the linear regression between the porosity ϕ_{MLR} and the laboratory permeability (k_{LAB}) has a $R^2 = 51\%$ and produces the equation:

$$\log(k_{LAB}) = -1.28574 + 6.62867\phi_{MLR}. \qquad (3)$$

Consequently, a multiple linear regression is choosing to evaluate a permeability. Figure 9 (right) presents these estimates using MLR and the total porosity derived from the density (track 3), neutron (track 4) and sonic (track 5) logs, and also for effective (track 6), LR (track 7) and MLR (track 8) evaluations, respectively. The expressions for the MLR with the different porosities have a general form:

$$\log(k_{MLR}) = $$
$$a + bGR + c\log(R_t) + d\varrho_b + e\phi_T + f\Delta_t, \qquad (4)$$
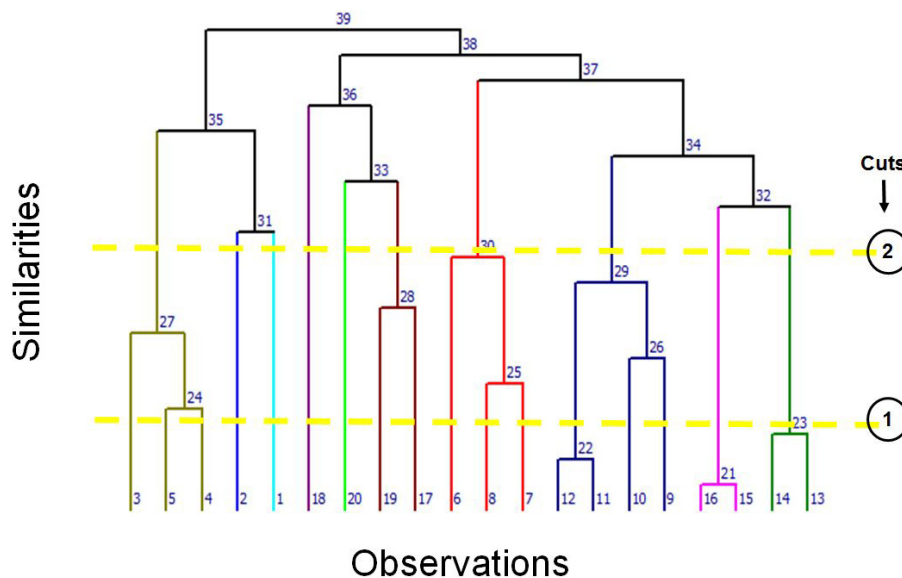
Figure 6 – Clusters in 10 different colors, considering density, neutron and sonic logs of well X, using the method of the sum of the square of the distance.
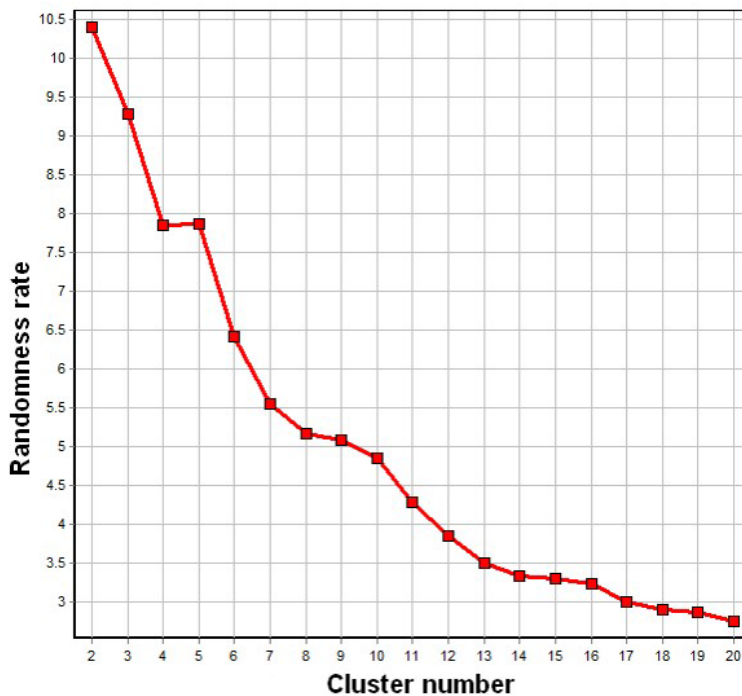
Figure 7 – Graph of randomness of the groups created by the k-means clustering.

where k_{MLR} is the MLR permeability, a, b, c, d, e and f are regression coefficients, as shown in Table 3 for each electrofacies, GR, R_t, ρ_b, ϕ_N and Δ_t is, respectively, the gamma ray, resistivity, density, neutron porosity and sonic logs. Again, it can say that the adjustment is good but that it is more mathematical than physical, because the value of the coefficient a, which represents a further regression coefficient, is larger than the coefficients b, c, d, e and f, which represent, respectively, the weight of GR, R_t, ρ_b, ϕ_N and Δ_t logs.

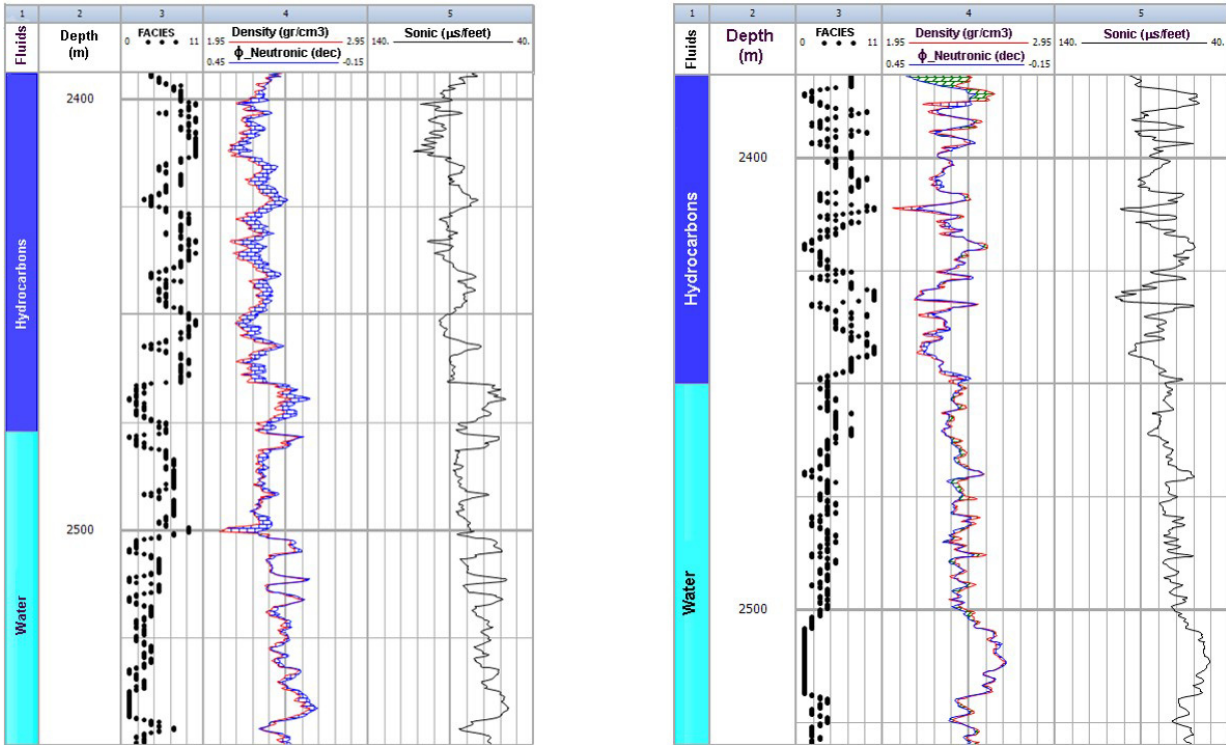**Figure 8** – In the third track electrofacies for well X (left) and well Y (right) for each depth.
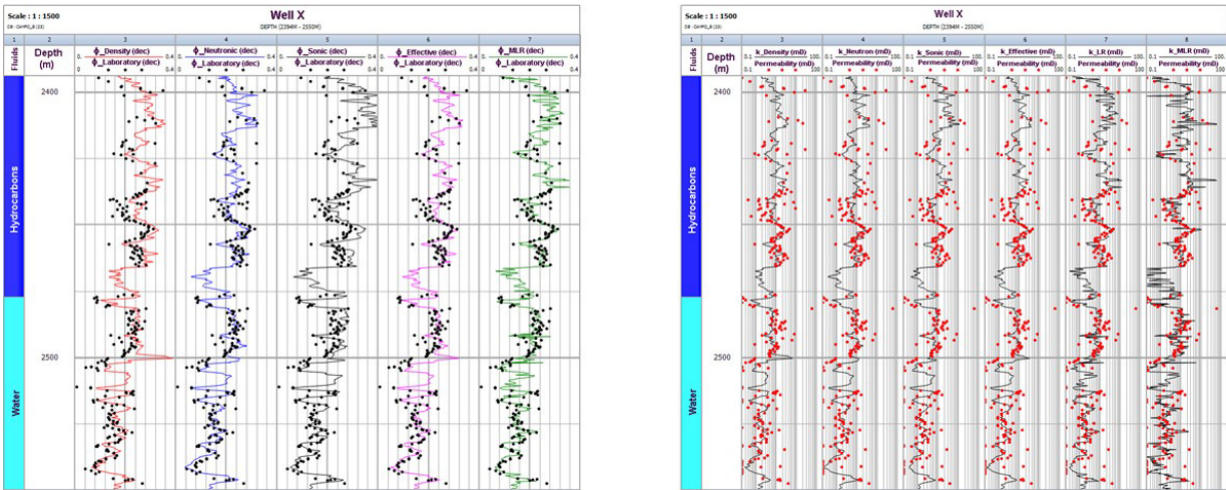

Figure 9 – Estimated values of porosity (left) and permeability (right) for well X compared with the respective data measured in the laboratory, using the estimates of density, neutron, sonic, effective, linear regression and multiple linear regression porosities.

Pickett (1966) plot proved to be similar in both wells, which served to estimate the value of the parameter m from the Archie Equation, by identifying in the crossplot resistivity *vs.* ϕ_{MLR} the points whose water saturation should be close to 100%. The red line in Figure 10 (left) represents approximately the position

within the reservoir with a water saturation of 100%. The slope of this line is a value of -2, whose absolute value is the value of $m = 2$, the cementation coefficient of Archie Equation. The point where this line intersects the porosity of 100% has a coordinate whose value is $R_w = 0.05$ ohm.m, which was verified using the

Table 2 – Regression coefficients for MLR porosity estimates.

Porosities			ρ_b	ϕ_N	Δ_t
Electrofacies	a	b	c	d	
1	1.2055	-0.3564	0.5000	0.0043	
2	-0.6399	-0.0160	-0.6600	0.0135	
3	-0.2125	0.0154	-0.7300	0.0063	
4	4.3099	-1.2922	0.2300	-0.0150	
5	2.1170	-1.2484	1.0100	0.0094	
6	0.5322	-0.1612	-0.1300	0.0009	
7	1.2964	-0.5461	-0.5300	0.0035	
8	1.0917	-0.5456	-0.0400	0.0004	
9	0.4966	0.0855	-0.2200	0.0060	
10	2.3843	-0.6172	-1.8500	-0.0023	

Table 3 – Regression coefficients for MLR permeability estimates.

Permeabilities		GR	R_t	ρ_b	ϕ_N	Δ_t
Electrofacies	a	b	c	d	e	f
1	-23.4417	0.1223	-0.0343	7.0065	0.0705	0.0570
2	-14.4223	0.0620	0.1343	-7.3135	0.0157	0.0270
3	-18.0389	-8.1711×10^{-4}	0.3595	5.6627	0.0304	0.0510
4	17.0906	-0.0200	0.1160	-4.7166	0.1284	-0.1074
5	20.9733	9.7409	-0.3767	-11.2586	0.0200	0.0714
6	2.6432	-0.0164	-0.1564	-0.6464	0.1374	0.0288
7	3.5692	0.0042	-0.2403	-2.8496	0.0454	0.0508
8	6.3893	0.0320	0.4359	-3.4814	0.0384	0.0136
9	-4.5946	0.0328	0.3521	1.5887	0.0458	0.0158
10	61.3056	-0.0648	-0.7212	-26.3540	0.1573	0.0320

Schlumberger (2013) charts. On the other hand, the volume of clay V_{SHALE}, with values below 20%, which corroborates that it is an Archie type reservoir, not being necessary to correct the porosity values. With all these values being calculated, the water saturation (S_W) can be calculated through Archie Equation, which is depicted in Figure 10 (right). In the upper part of this figure, it was observed, S_W with values less than 10% in the upper portion where the hydrocarbons are. At the bottom, S_W values of up to 100% appear, which is the portion of the aquifer. Between these two areas, the transition area is, with S_W values changing with depth.

The best correlation between calculated porosity and permeability data and laboratory data using multiple linear regression it was used to generate the Winland (1972) graphic. Figure 11a shows three flow units in Albian reservoir of well X and pore throats with values lower than 4 mm, as shown by the red lines in this chart. The first flow unit (red dash line) is characterized

by having micro pores, pore throats between 0.01 and 0.1 mm, total porosity around 10% and permeability around 0.5 mD. The second (blue dash line) has micro pores and meso pores, pore throats between 0.07 and 0.1 mm, total porosity around 20% and low permeability around 1 mD. The third (green dash line) presents meso pores, pore throats between 0.05 and 1 mm (blue dash line), total porosity around 30%, permeability around 10 mD and high oil saturation, thus constituting itself in the unit with better characteristics for hydrocarbon production. With small variations, the same values are found for well Y in Figure 11b, allowing the identification points which the porosity and permeability have incorrectly calculated by multiple linear regression.

Figures 12 and 13 show a summary of the petrophysical characterization results found for well X (Fig. 12) and well Y (Fig. 13). In these figures, are shown the values for facies (track 3), pore throats (track 4), flow units (track 5), GR, V_{SHALE} and S_W logs (track 6), R_t log (track 7), ρ_b and ϕ_N logs (track 8), Δ_t
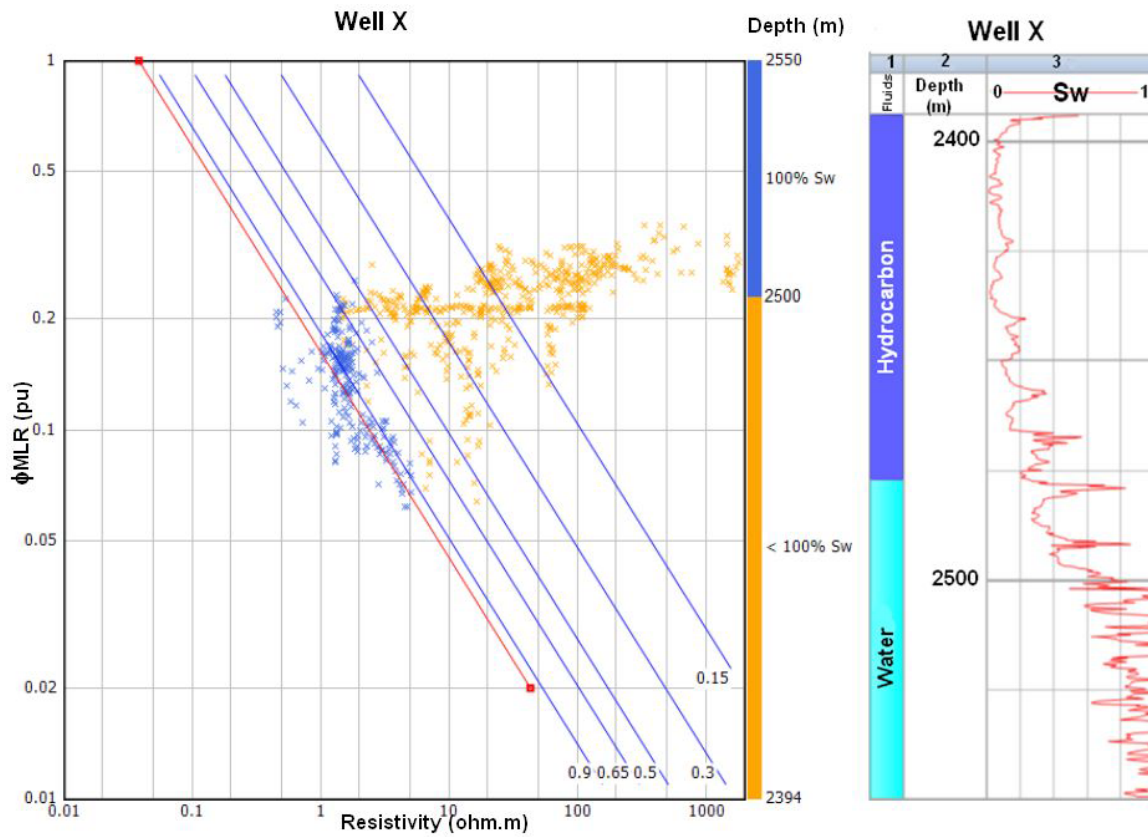
Figure 10 – Pickett graph for well X of the Oilfield B, with light blue indicating the aquifer and dark blue zone hydrocarbon. Slopes of the straight lines are the parameter m of Archie Equation ($m = 2$).
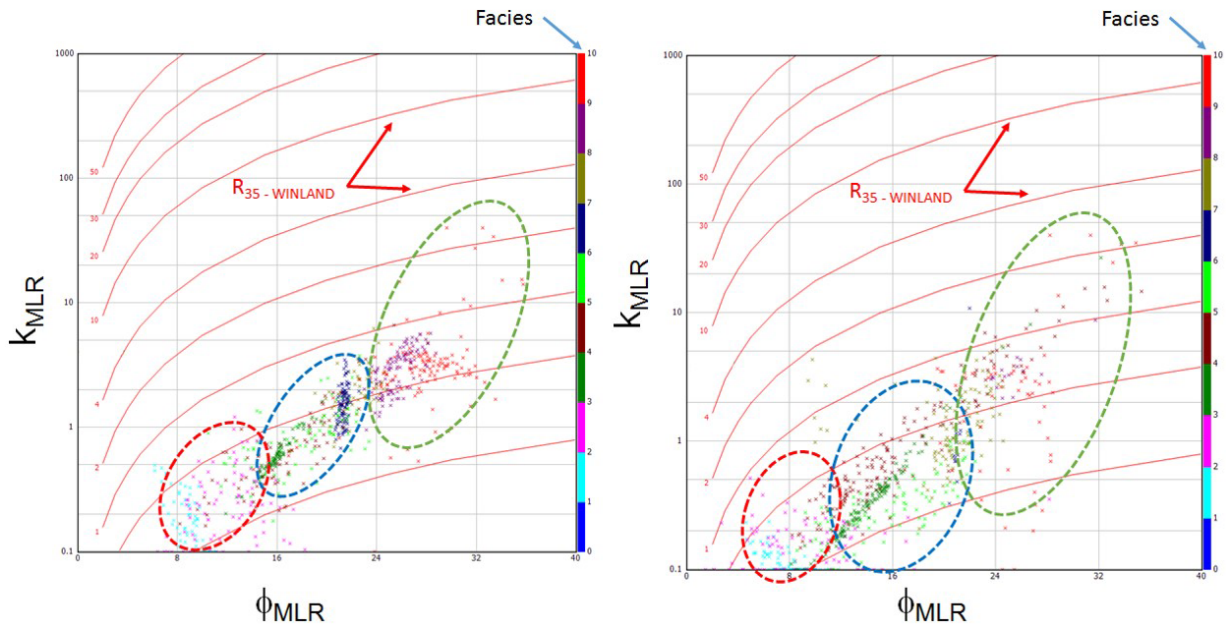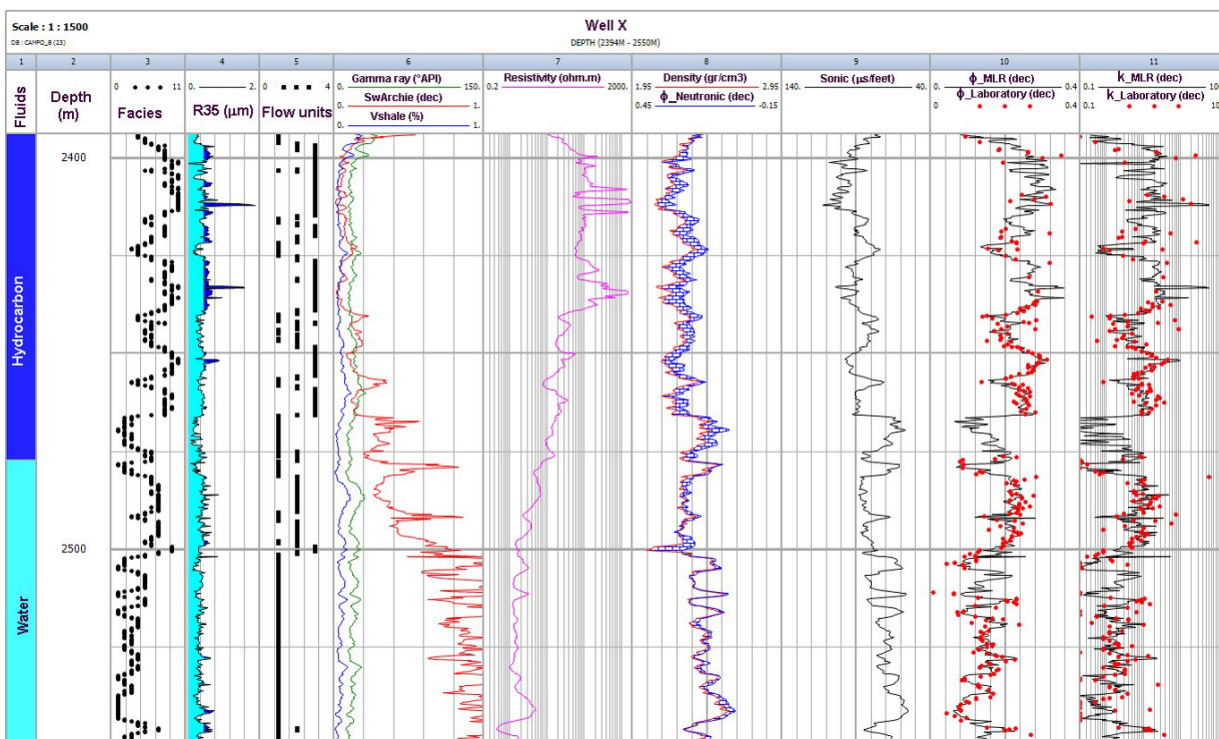

Figure 11 – Winland graph for well X (left) and well Y (right) of the Oilfield B, where the different colors mean different electrofacies, red curves are the pore throat radius and ellipses mean flow zones, with red being the zone 1, blue the zone 2 and green the zone 3.

Figure 12 – Full interpretation for well X, highlighting the electrofacies in the third track, the pore throat radius in the fourth, the flow units in the fifth and water saturation and volume of clay in the sixth track.
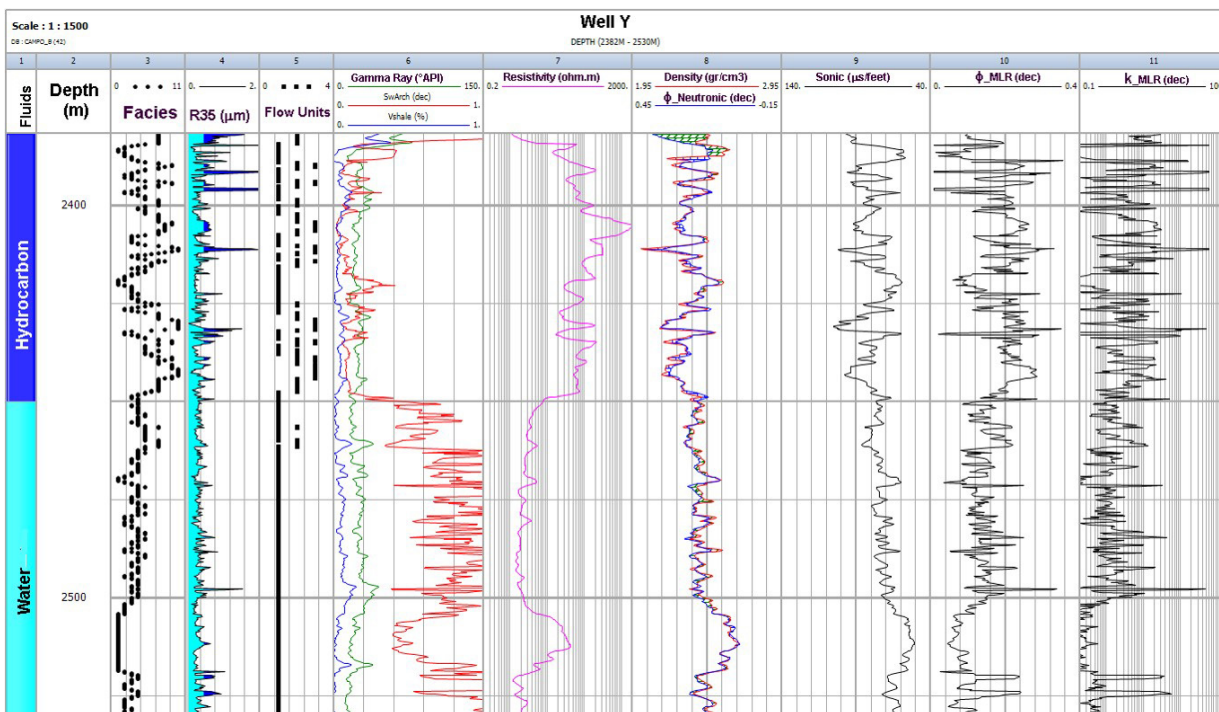
Figure 13 – Full interpretation of the well Y, highlighting electrofacies in the third track, the pore throat radius in the fourth, flow units in the fifth and water saturation and volume of clay in the sixth track.

log (track 9), ϕ_{MLR} together with ϕ_{LAB} (track 10), and k_{MLR} together with k_{LAB} (track 11). For the two wells, the best part of the reservoir between depths 2400 and 2460 m for well X (Fig. 12) and 2375 and 2450 for well Y (Fig. 13). These depths are characterized by having facies values greater than 9 (track 3), pore throats larger than 0.4 mm (dark blue on track 4), flow units larger than 2 (track 5), low values of $GR < 20\%$, $V_{SHALE} < 10\%$ and $S_W < 15\%$ (track 6), R_t log with values up to 1000 ohm.m showing the presence of hydrocarbons (track 7), cross between ρ_b and ϕ_N logs which probably indicates the presence of gas (blue shading on track 8), Δ_t log with values for around 80 us/ft (track 9), ϕ_T above 25% (track 10) and k above 10 mD (track 11).

CONCLUSIONS

In this work, logs and laboratory data allowed to estimate the porosity of well X of an Albian carbonate reservoir of Field B using different approaches. The different porosity curves present similar behavior, with a characteristic oscillation in this kind of reservoirs, indicating a good (between 10% and 20%) or excellent (above 20%) porosity in the portion of interest of the well. Among the different techniques used to calculate porosity, the combination of the Cluster Analysis for Rock Typing module of the Interactive Petrophysics software and the multiple linear regression technique presented the best result with a coefficient of determination of 75%. To characterize the water saturation, the Archie (1942) Equation was used after identifying that the clay was low (less than 20%) and cementation coefficient $m = 2$ in both wells in its zones of interest. well X showed low water saturation (less than 15%) in the hydrocarbon region, intermediate (between 15% to 60%) in the transition zone and high (between 60% and 100%) in the water zone. The permeability was estimated using linear regression and multiple linear regression techniques after identifying that there was a correlation between the porosity and the permeability measured in the laboratory in well X. The equations defined with the laboratory data from well X showed permeability varying between poor (less than 1 mD) and reasonable (between 1 mD and 5 mD) in the zone of interest. As in the porosity calculation, the combination of Cluster Analysis for Rock Typing with multiple linear regression showed a better correlation with well X laboratory data with a determination coefficient of 62%. Finally, the porosity and permeability data with better correlation with the laboratory data were used to generate the Winland (1972) graph, which allowed to identify the flow units. Three flow units were identified in the reservoir. The first is present in the water zone and is characterized by having micro pores, good porosity (between 8% and 24%) and poor permeability (between 0.1 m

and 1 mm mD). The second is present in the transition zone and has micro pores and meso pores, good porosity (between 16% and 24%) and reasonable permeability (between 0.7 mD and 4 mD). The third is present in the hydrocarbon zone and presents meso pores, excellent porosity (between 24% and 32%) and reasonable permeability (between 2 mD and 5 mD). This is the unit with the best characteristics for production of hydrocarbons. The methodology assumed in the characterization of well X was extended to well Y, reaching the same success in the petrophysical estimates.

REFERENCES

AGUILERA R & AGUILERA M. 2001. The integration of capillary pressures and Pickett plots for determination. In: SPE Annual Technical Conference and Exhibition, New Orleans, SPE-71725-MS.

ARCHIE G. 1942. Electrical resistivity log as an aid in determining some reservoir characteristics. Trans. AIME, 146: 54–62.

BRUHN C, GOMES J, LUCCHESE C & JOHANN P. 2003. Campos basin: reservoir characterization and management – Historical overview and future challenges. In: Offshore Technology Conference, Houston, paper OTC 15220, 14 pp.

BURROWES A, MOSS A, SIRJU C & PRITCHARD T. 2010. Improved permeability prediction in heterogeneous carbonate formation. In: SPE EUROPEC/EAGE Annual Conference and Exhibition, Barcelona, SPE-131606-MS.

LR SENERGY. 2014. Interactive Petrophysics v4.3, Online User's Manual. Available on: <http://www.lr-senergy.com/software/ip>. Access on: March 11, 2015.

LUCIA F. 1999. Carbonate Reservoir Characterization. Springer-Verlag, Berlin, 226 pp.

OKUBO J, LYKAWKA R, WARREN LV, FAVORETO J & DIAS-BRITO D. 2015. Depositional, diagenetic and stratigraphic aspects of Macaé Group carbonates (Albian): example from an oilfield from Campos Basin. Brazilian Journal of Geology, 45(2): 243–258.

PICKETT G. 1966. A Review of current techniques for determination of water saturation from logs. Journal of Petroleum Technology, 18: 1425–1433.

SCHLUMBERGER. 2013. Log interpretation charts. Educational Services. USA, 306 pp.

SHENAWI S, WHITE J, ELRAFIE E & EL-KILANY K. 2007. Permeability and water saturation distribution by lithologic facies and hydraulic units: a reservoir simulation case study. In: SPE Middle East Oil and Gas Show and Conference, Manama, SPE-105273-MS.

SILVA R. 2016. Petrophysical characterization of an Albian carbonate reservoir using well logs and laboratory measurements. Master Thesis, UENF/CCT/LENEP, Macaé – RJ, Brazil, 157 pp. (In Portuguese).

TIAB D & DONALDSON E. 2004. Petrophysics: theory and practice of measuring reservoir rock and fluid transport properties. Elsevier. 918 pp.

WINLAND H. 1972. Oil accumulation in response to pore size changes, Weyburn field. Saskatchewan: Amoco Production Company Report F72-G-25, 20 pp. (Unpublished).